Korean J. Chem. Eng., 32(1), 30-36 (2015)
DOI: 10.1007/s11814-014-0175-3

pISSN: 0256-1115
eISSN: 1975-7220

Bubble point measurement and high pressure distillation column design for the environmentally benign separation of zirconium from hafnium for nuclear power reactor

Le Quang Minh*, Gyeongmin Kim*, Jongki Park, and Moonyong Lee*,†**

*School of Chemical Engineering, Yeungnam University, Gyeongsan 712-749, Korea
**Korea Institute of Energy Research, Daejeon 305-343, Korea
(*Received 10 April 2014 • accepted 24 June 2014*)

Abstract−We examined the feasible separation of $ZrCl_4$ and $HfCl_4$ through high pressure distillation as environmentally benign separation for structural material of nuclear power reactor. The bubble point pressures of $ZrCl_4$ and $HfCl_4$ mixtures were determined experimentally by using an invariable volume equilibrium cell at high pressure and temperature condition range of 2.3-5.6 MPa and 440-490 °C. The experimental bubble point pressure data were correlated with Peng-Robinson equation of state with a good agreement. Based on the vapor-liquid equilibrium properties evaluated from the experimental data, the feasibility of high pressure distillation process for the separation of $ZrCl_4$ and $HfCl_4$ was investigated with its main design condition through rigorous simulation using a commercial process simulator, ASPEN Hysys. An enhanced distillation configuration was also proposed to improve energy efficiency in the distillation process. The result showed that a heat-pump assisted distillation with a partial bottom flash could be a promising option for commercial separation of $ZrCl_4$ and $HfCl_4$ by taking into account of both energy and environmental advantages.

Keywords: Zirconium Tetrachloride, Hafnium Tetrachloride, Nuclear Power Reactor, Bubble Point Pressure, Peng-Robinson Equation of State, High Pressure Distillation, Heat Pump

INTRODUCTION

Zirconium (Zr), with some minor alloy addition, is used as core structural material in nuclear power reactors owing to its low thermal neutron cross section, excellent high temperature strength, and resistance to corrosion in water [1]. Hafnium (Hf), however, which can be found in zirconium ore at 1-3 wt% in a state of nature, should be removed completely from Zr because of its high thermal neutron cross section. The concentration of Hf in the purified Zr should be less than 100 ppm for the nuclear power reactor application, while the separation of these elements is quite challenging because of their similar physical and chemical properties with almost identical ionic radii [2], which necessitates a novel chemical processing step for producing Hf-free Zr in the commercial nuclear reactor applications.

Several methods have been proposed for Zr-Hf separation, such as crystallization, fused salt electrolysis and extraction [3-5]. Among them, so far, the most popular and economic way for commercial purpose Zr-Hf separation is extraction. In most extraction based Zr-Hf separations, the crude tetrachloride is converted to a mixture of their oxychlorides, and is then processed using a multiple-step solvent extraction process in the presence of solvent. The equipment and processing entailed encompass a large portion of the entire processing facility for the production of Zr and Hf metals. Nevertheless of its main advantages in mass production, the extraction-based Zr-Hf separation entails considerable amounts of relatively expensive, corrosive and environmentally harmful solvent chemicals. The process also generates a huge volume of liquid waste, which is difficult to dispose due to the stringent environmental protection laws [6-11]. For example, the most popular solvent used for Zr-Hf extraction is isobutyl methylketone (MIBK), which requires environmentally harmful cyanogen (CN) chemicals as an additive.

To overcome this environmental limitation, distillation-based direct separations of $ZrCl_4$ and $HfCl_4$ have recently got the attraction as tetrachlorides are the starting intermediate for the Kroll reduction to metal Zr and Hf [12]. Distillation has been most widely used in process industries as a clean separation technique without introducing any third material as well as its many other advantages for large scale production. However, since distillation utilizes volatility difference of the components associated with vapor-liquid equilibrium, both a narrow region of vapor-liquid phase and close boil-

Table 1. Physical properties of zirconium and hafnium tetrachlorides [13]

Properties	$ZrCl_4$	$HfCl_4$
Sublimation temperature (°C)	331	317
Triple point		
Temperature (°C)	437	432
Pressure (bar)	22.36	45.01
Critical point		
Temperature (°C)	506	499
Pressure (bar)	57.66	57.76
Volume (ml/mol)	319	303

†To whom correspondence should be addressed.
E-mail: mynlee@yu.ac.kr

ing point difference in $ZrCl_4$ and $HfCl_4$ are a main obstacle to its commercial application for Zr-Hf separation. Table 1 lists the properties of $ZrCl_4$ and $HfCl_4$ [13]. $ZrCl_4$ and $HfCl_4$ directly sublime at 331 and 317 °C at ambient pressure, respectively. Their vapor pressures are 22.36 and 45.01 bar at the triple points of 437 °C and 432 °C, respectively, which easily approach to their critical condition as the temperature increases. The temperature range for the existence of vapor-liquid phase, which is essential for the separation of $ZrCl_4$ and $HfCl_4$ mixtures through distillation, is relatively narrow. Because of this limitation, few attempts have been made to separate $ZrCl_4$ and $HfCl_4$ by distillation under high pressure conditions [14,15]. The lack of accurate vapor-liquid equilibrium data is another obstacle that prevents the precise design of a commercial distillation column to separate $ZrCl_4$ and $HfCl_4$.

In this study, the experimental bubble point pressures for a $ZrCl_4$-$HfCl_4$ mixture system were investigated. The experimental data was correlated to determine the acentric factors and interaction parameter, which were then embedded into the used equation of state in a commercial process simulator. The feasibility of high pressure distillation was investigated for the separation of $ZrCl_4$ and $HfCl_4$ with its main design condition through rigorous simulation. A heat pump-assisted enhanced distillation configuration was also examined to improve the energy efficiency of the distillation process further.

EXPERIMENTAL

1. Chemicals

$ZrCl_4$ and $HfCl_4$ were obtained from the Alfa Aesar, Johnson Matthey Catalog Company with a certified purity of 99.5 wt% and 99.9 wt%, respectively. $ZrCl_4$ and $HfCl_4$ must be kept in a moisture-free closed system because of their high hygroscopic sensitiv-

Fig. 1. Experimental apparatus for determining the bubble point pressure of a binary mixture.

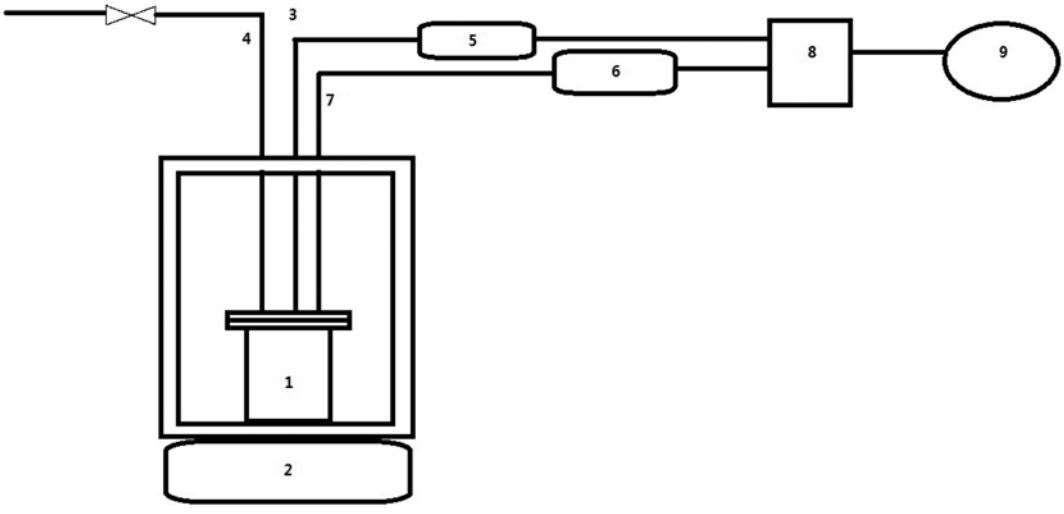

Fig. 2. Schematic diagram for measuring the bubble point pressure.

1. Equilibrium cell
2. Electric furnace
3. Thermocouple sensor
4. Inert gas inlet
5. Temperature indicator
6. Pressure gauge
7. Pressure sensor
8. NI box
9. Computer

ity. During sample preparation, all procedures should be carried out in a glove box system.

2. Experimental Apparatus and Technique

Experimental equipment (Fig. 1) was developed for precise measurement of bubble point pressures as a function of temperature for $ZrCl_4$ and $HfCl_4$ mixtures of known overall composition. A schematic diagram for the bubble point measurements is shown in Fig. 2. The pressure conditions of the fluid were measured with an accuracy of 1 mbar. The temperature near the top of the cell is read by a thermometer ranging from −55 °C to 538 °C. The heart of the apparatus is an invariable volume cell designed for the high pressure and temperature resistance. The stainless steel cell has dimensions of 45 mm I.D×70 mm O.D with an internal working volume of 150 cm^3. An electric furnace with the maximum temperature capacity approaching 1,200 °C was used to achieve the high temperature condition required.

All procedures of sample preparation were carried out in a glove box to avoid the hygroscopic phenomenon. After preparing the sample, a cell cover with a thermocouple and a pressure sensor were assembled with a main cell in the glove box system. A metal graphite O-ring was used in the flange to prevent gas leakage at high temperature and pressure condition. After the cell was assembled, the system was placed inside the electric furnace to carry out the experiment.

Once the cell was implemented in the furnace, the apparatus was gradually heated and helium gas was constantly input into the cell at the initial point to maintain a positive pressure inside the cell until 150 °C. During the heating steps, both ends of the cell were slightly hotter than the center section. This is necessary to prevent possible condensation of $ZrCl_4$ and $HfCl_4$ vapor on these parts that can cause a severe problem in the high pressure gauge. The temperature and pressure readings were taken at approximately 10 °C increments with the temperature maintained at each point until no pressure fluctuations were noted.

Both temperature and pressure values were recorded using a NI™ box. The signal from the NI™ box was interfaced with a computer using LABVIEW™ 8.6 software. The liquid compositions of each experimental point were calculated from the feed composition by correcting the mass of each component existing in the vapor phase.

RESULTS AND DISCUSSIONS

1. Vapor Pressure of Pure $ZrCl_4$ and $HfCl_4$

Proper modeling and interpretation of the experimental phase equilibrium data for binary systems require knowledge of the pure component properties, particularly the vapor pressure [16]. In this study, the vapor pressures of pure liquid $ZrCl_4$ and $HfCl_4$ were measured at temperatures ranging from 440 °C to 490 °C using the experimental apparatus described in the previous section. Table 2 lists the resulting vapor pressure values of each substance. The vapor pressure of $HfCl_4$ was reasonably higher than that of $ZrCl_4$ as expected. This observation was also reported elsewhere but for the sublimation vapor pressure [17-20]. The volatility of $HfCl_4$ was approximately 1.7 times higher than that of $ZrCl_4$ in the range of investigated temperatures, which revealed the feasibility of economic separation of $HfCl_4$ and $ZrCl_4$ by high pressure distillation.

Table 2. Vapor pressure data of pure $ZrCl_4$ and $HfCl_4$

Temperature (°C)	Vapor pressure (bar)	
	$ZrCl_4$	$HfCl_4$
440	23.32	45.92
450	26.83	48.06
460	30.94	49.12
470	35.34	51.94
480	40.63	53.78
490	46.52	55.34

The vapor pressures of pure $ZrCl_4$ and $HfCl_4$ were correlated with the Clapeyron equation as:

$$\log_{10} p_{ZrCl_4} = \frac{-3260}{T} + 8.814 \quad (1)$$

$$\log_{10} p_{HfCl_4} = \frac{-895}{T} + 5.793 \quad (2)$$

where P and T denote vapor pressure in mmHg and temperature in K, respectively.

Fig. 3 compares the experimental vapor pressure and the regressed vapor pressure lines by Eqs. (1) and (2). As shown, the correlated vapor pressure lines showed a good agreement with their experimental values.

The Peng Robinson equation of state (PR-EOS) was selected to predict the vapor liquid equilibrium (VLE) behavior of a $ZrCl_4$ and $HfCl_4$ mixture system. The vapor pressure data of pure $ZrCl_4$ and $HfCl_4$ was also used to correlate the acentric factor in the PR-EOS (this will be discussed in the next section).

2. Bubble Point Calculation of the System

The use of a simple EOS to evaluate the VLE behavior is preferred over the use of a more complicated model, particularly for high pressure systems [21]. The PR-EOS was selected because of its proven performance in high pressure condition and the non-ideal/

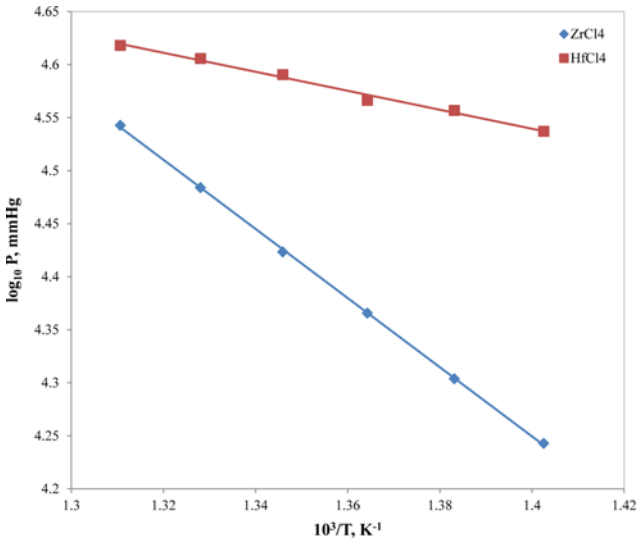

Fig. 3. Vapor pressure of $ZrCl_4$ and $HfCl_4$.

non-polar characteristics of the $ZrCl_4$ and $HfCl_4$ mixture [22-26].

The standard PR-EOS was expressed as following equations [26]:

$$P = \frac{RT}{v-b} - \frac{a}{v(v+b)+b(v-b)} \quad (3)$$

$$\text{where } a(T) = \frac{0.45724R^2T_C^2}{P_C}\alpha(T) \quad (4)$$

$$b = \frac{0.07780RT_C}{P_C} \quad (5)$$

with

$$\alpha(T)=(1+m(1-T_r^{0.5}))^2 \quad (6)$$

$$m=0.37464+1.54226\omega-0.26992\omega^2 \quad (7)$$

The constants a and b can be calculated using the critical properties. The parameter m can be determined from the acentric factor. In this study, the acentric factor of pure $ZrCl_4$ and $HfCl_4$ was obtained via the regression by minimizing the objective function given in Eq. (8) from the vapor pressure data of the corresponding pure substance.

$$\text{Obj.} = \sum_{i=1}^{N}\left(\frac{p_i^{exp}-p_i^{cal}}{p_i^{exp}}\right)^2 \quad (8)$$

where and are the experimental pressure and the calculated pressure by the EOS prediction, respectively.

The resulting acentric factor values were 1.012 and −0.5163 for $ZrCl_4$ and $HfCl_4$, respectively.

When considering multi-component systems, mixing rules have to be applied to determine the mixture constants a and b as follows [26]:

$$a_{mix} = \sum_i \sum_j z_i z_j a_{ij} \quad (9)$$

$$a_{ij}=(a_i a_j)^{0.5}(1-k_{ij}) \quad (10)$$

$$b_{mix} = \sum_i z_i b_i \quad (11)$$

where z_i is the liquid or vapor phase mole fraction.

In Eq. (10), the binary interaction parameter k_{ij} can also be determined by minimizing the objective function by Eq. (8), using the experimental bubble point pressure data of $ZrCl_4$ and $HfCl_4$ mixtures. In this study, because of the dependence of the operating temperature range, the value of k_{ij} was determined over the entire temperature range. The resulting optimal value for k_{ij} was 0.0135 with a sufficiently small root mean square error. Using the k_{ij} parameter obtained, the composition of vapor phase was calculated at the specific liquid fraction by solving the following equilibrium relations simultaneously,

$$y_i\hat{\phi}_i^v = x_i\hat{\phi}_i^l \text{ for i=1, 2} \quad (12)$$

where $\hat{\phi}_i^v$ and $\hat{\phi}_i^l$ are the fugacity coefficients of component i in the mixture in the vapor and liquid phases, respectively.

3. Bubble Point Results and Discussion

The bubble point pressure at a given temperature and liquid composition is defined as the initial pressure at which the first bubble begins to form. The procedure for the measurement of a bubble point was described previously. The numerical values of the experimental data for the $ZrCl_4$-$HfCl_4$ mixture are plotted in Fig. 4. Due to the temperature limitation, the experiment was investigated carefully to avoid an excess of critical pressure. As the system temperature increases, the bubble point pressure increases and finally ends up at the critical point of the mixture. The results show that increasing the $HfCl_4$ composition in the mixture leads to an increase in the bubble point pressure of the mixture.

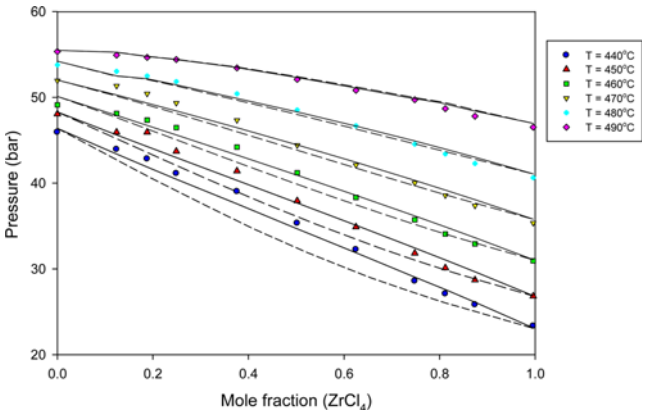

Fig. 4. P-xy diagram at different temperatures for the $ZrCl_4$/$HfCl_4$ system: the symbols denote experimental bubble points, and the solid and dashes lines are the bubble point and dew point curves correlated by the PR-EOS, respectively.

The root mean square error (RMSE) defined by Eq. (13) with the resulting regressed value for k_{ij} was small enough as 2.34, which showed an accuracy of the prediction for the selected model.

$$\text{RMSE} = \sqrt{\frac{\sum_{i=1}^{n}(p_{i,exp}^{bubble}-p_{i,cal}^{bubble})^2}{n}} \quad (13)$$

where $p_{i,cal}^{bubble}$ is the experimental bubble point pressure corresponding to the i^{th} experimental data, whereas $p_{i,exp}^{bubble}$ is the calculated pressure by the EOS model under the same condition.

The relatively small value of k_{ij} indicates a minor deviation from ideal behavior in the liquid phase, which is also confirmed by the occurrence of an almost linear dependence of the various bubble point curves with the $ZrCl_4$ mole fraction (Fig. 4). Furthermore, at higher temperatures, the relative volatility tends to be smaller through two adjacent lines of the bubble point curve and dew point curve. Consequently, the separation of a binary mixture becomes stricter due to the limited range of temperatures. Note that although the results of the bubble calculated by the PR-EOS showed a reasonably good agreement with their experimental values, the dew points estimated by the PR-EOS are not confirmed to be accurate.

DESIGN OF HIGH PRESSURE DISTILLATION PROCESS

A conceptual design study of high pressure distillation was done to investigate the main design conditions as well as its feasibility for the separation of $ZrCl_4$ and $HfCl_4$ for nuclear power reactor

Table 3. Feed condition and product specification

	Values
Feed: Composition (%wt)	
$ZrCl_4$	98.4
$HfCl_4$	1.6
Molar flow (kmol/h)	100
Temperature (°C)	460
Pressure (bar)	32.5
Product specification:	
Mass fraction of $HfCl_4$ at the bottom stream	<40 ppm
Recovery of $ZrCl_4$ (%)	>85

application. The design was examined for a crude feed mixture consisting of 98.4 wt% $ZrCl_4$ and 1.6 wt% $HfCl_4$. The distillation process was designed to obtain an ultra-purified $ZrCl_4$ with 40 ppm $HfCl_4$ concentration and a $ZrCl_4$ recovery of 85%. Table 3 lists the feed condition and product specification used in the column design. In addition to the conventional distillation, a heat pump assisted configuration was also studied to enhance the energy efficiency of distillation further.

1. Conventional Distillation Column

A flow sheet of the conventional distillation column is shown in Fig. 5 with its main design condition. The flow rate of the feed stream was supplied at 100 kmol/h. The PR-EOS model with the regressed parameters from the experiment was applied to simulate the process in ASPEN HYSYS 8.4. Due to the missing parameters of pure component in the HYSYS database, the hypothetical-component definition was implemented through using the k_{ij} parameter obtained. The column was initially set up using the short-cut column design facility to obtain an estimate for the required number of trays and the needed reflux ratio in the column. The column was then simulated rigorously to find the optimal design condition. Good results were obtained when using the conditions based on a column base temperature of at least 455 °C. Local cooling effects resulted in occasional freezing of the system when a lower pressure was maintained so that the column base temperature fell to approximately 445 °C. On the other hand, at higher temperatures, the column efficiency began to fail. This was attributed to the proximity to the critical temperature where the relative volatility decreases rapidly. Therefore, the column has to be operated at least at 30 bar and 460 °C to avoid solidification. Pure $ZrCl_4$ with the required product specification was obtained from the bottom section of the column. The material of construction should be chosen considering high pressure and temperature condition. In the present study, CS+SUS321 cladding was recommended for enduring the high pressure and temperature condition in an economic way while avoiding possible metal deposition from the column structure.

For the optimization of column structure, the number of stages was varied while keeping the product specifications. Fig. 6 shows the relationship between the number of stages and the total energy requirement (condenser and reboiler duty). Based on this sensitivity analysis, the optimal number of trays in the column was selected at 155. In addition, the column was designed with the maximum flooding of approximately 80% to prevent flooding in the column. To determine the maximum flooding of a particular column, the rating mode was simulated using the column internal specifica-

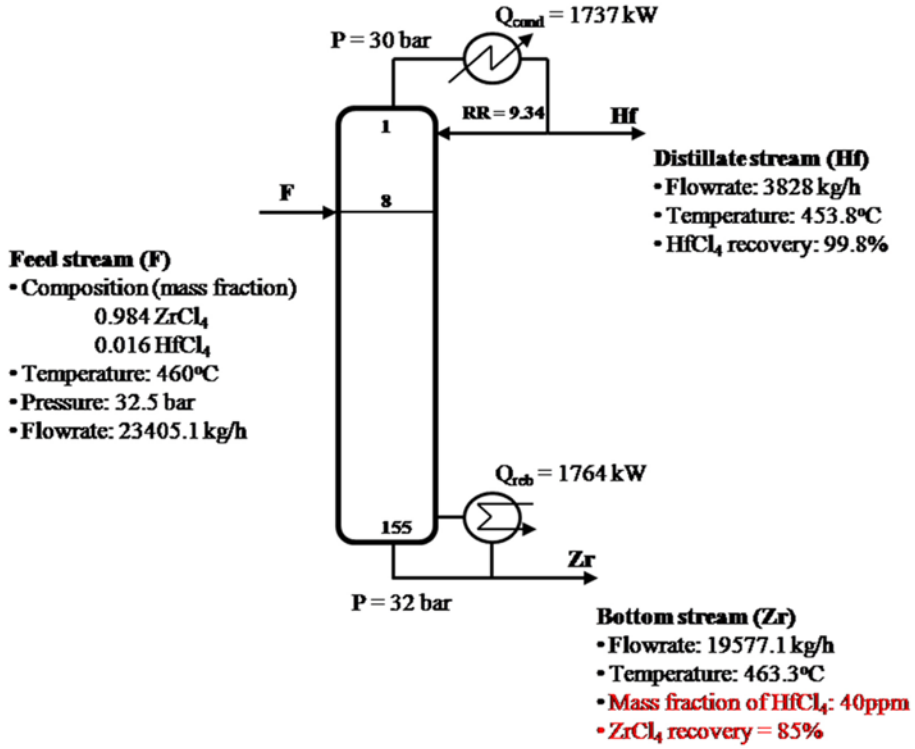

Fig. 5. A flow sheet diagram illustrating the high pressure distillation column.

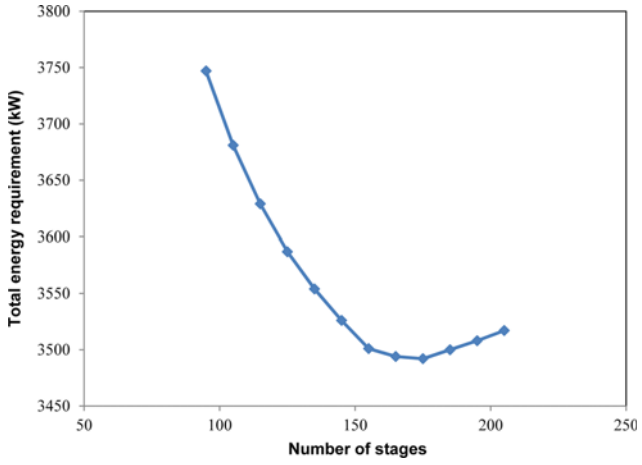

Fig. 6. Sensitivity analysis between the number of stages and the total energy requirement for the high pressure distillation column.

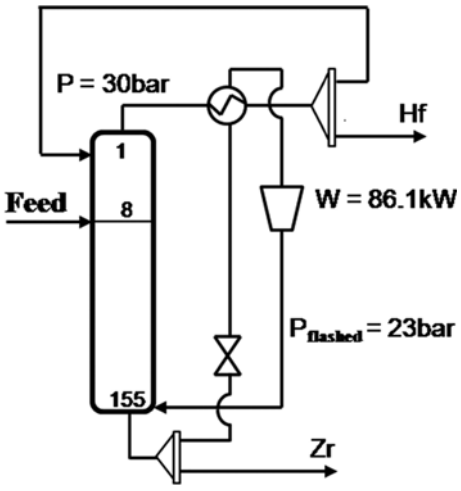

Fig. 7. A flow sheet diagram illustrating the partial bottom flashing heat pump.

Table 4. Hydraulic condition and energy performance for the conventional column

Number of trays	155
Feed tray	8
Tray type	Packed
Column diameter (m)	0.85
Max flooding (%)	74.27
Energy requirement of condenser (kW)	1737
Energy requirement of reboiler (kW)	1764

Table 5. Comparison of different structural alternatives for more efficient ultra-purification

Structure alternative	Conventional column	Distillation with partial bottom flashing heat pump
Tray number	155	155
Column diameter (m)	0.85	0.85
Condenser duty (kW)	1737.0	0
Compressor duty (kW)	0.0	86.1
Reboiler duty (kW)	1764.0	0.0
Condenser duty saving (%)	0.0	100.0
Reboiler duty saving (%)	0.0	95.1

tions. Table 4 lists the parameters needed to define the existing hydraulic features and energy performance of the column. Due to the high reflux ratio of the column, the required reboiler duty turned out somewhat high such as 90 W per 1 kg/hr Zr production. Furthermore, a fuel furnace should be used as a high temperature generation source to boil up the bottom section of the column. Simultaneously, in view of economic advantage, the latent heat from top vapor condensation could be utilized to generate high pressure steam.

2. Enhanced Configuration with Heat-pump Technique

Heat pump technology is an economic way to conserve energy when the temperature difference between the overhead and bottom of the column is small enough and the heat load is high. Popular heat pump assisted methods include top vapor recompression, closed cycle heat pump, and bottom flashing heat pump [27]. Many studies have been developed to improve the heat pump technology for a given application [28-31]. In this study, the focus was mainly on the feasibility of the enhanced configuration by partial bottom flashing heat pump.

In the partial bottom flashing heat pump configuration, the bottom stream from the convention column is divided into two streams: the bottom product stream and another that is flashed until its dew point temperature lower than the overhead temperature. Fig. 7 presents a schematic diagram of partial bottom flashing configuration for this study. The flashed pressure from the valve was adjusted 23 bar to obtain the minimum approach in the heat exchanger of 10 °C [28]. The boilup stream is recompressed back to the column pressure after the heat exchanger. The result showed that using a partial bottom flashing heat pump can drastically reduce energy requirement by up to 100.0% and 95.1% in the condenser and reboiler duty, respectively, compared with the conventional distillation column. The required reboiler duty is reduced down to only 4.4 W per 1 kg/hr Zr production. A comparative summary of the key results is listed in Table 5.

CONCLUSIONS

The bubble point pressures for $ZrCl_4$ and $HfCl_4$ mixture were investigated experimentally within the temperature range from 440 and 490 °C using an invariable volume cell. The experimental data were correlated with the PR-EOS with a good agreement. Several essential parameters for the PR-EOS were obtained: the acentric factor w of $ZrCl_4$ and $HfCl_4$ as 1.012 and –0.5163, respectively, and the binary interaction parameter k_{ij} of $ZrCl_4$-$HfCl_4$ mixture as 0.0135.

The distillation process was designed through rigorous simulation to obtain an ultra-purified $ZrCl_4$ less than 40 ppm $HfCl_4$ impurity and more than 85% $ZrCl_4$ recovery. The main design condition confirmed the feasibility of distillation for $ZrCl_4$-$HfCl_4$ separation. Furthermore, it turned out that a partial bottom flashing heat pump

configuration could be an attractive option to reduce the energy requirement drastically: it reduced energy requirement by up to 95.1% in reboiler duty compared with the conventional column.

In conclusion, although there are still several practical issues for its commercial application, the high pressure distillation with the enhanced configuration can be a promising option for high purity $ZrCl_4$-$HfCl_4$ separation in an environmentally benign and economic way.

ACKNOWLEDGEMENTS

This study was supported by a grant from the Fundamental R&D Program for Integrated Technology of Industrial Materials funded by the Ministry of Knowledge Economy, Republic of Korea. This study was also supported by Basic Science Research Program through the National Research Foundation of Korea (NRF) funded by the Ministry of Education, Science and Technology (2012012532).

REFERENCES

1. D. G. Franklink and P. M. Lang, *Zirconium – Alloy Corrosion: A review based on an IAEA meeting, In Zirconium in Nuclear Industry, Ninth International Symposium*, Philadelphia, 3 -32 (1991).
2. D. Sathiyamoorthy, S. M. Shetty, D. K. Bose and C. K. Gupta, *High Temp. Mater. Processes*, **18**, 213 (1999).
3. Annual Book of ASTM Standards: part 8, Nonferrous Metals-Nickel, Lead and Tin Alloys, Precious Metals, Primary Metals; Reactive Metals, *American Society for Testing and Materials*, Philadelphia (1976).
4. L. Moulin, P. Thouvenin and P. Brun, *Paper presented at the 6th international conference on zirconium in the nuclear industy*, Vancouver, B.C., Canada (1982).
5. D. J. Branken, *M.S. Thesis*, North-West University (2009).
6. I. V. Vinarov, *Russ. Chem. Rev.*, **36**, 522 (1967).
7. R. Tricot, *J. Nucl. Mater.*, **189**, 277 (1992).
8. L. Moulin, P. Thouvenin and P. Brun, *ASTM Spec. Tech. Publ.*, **284**, 37 (1984).
9. E. D. Lee and D. F. McLaughlin, US Patent, 4,913,778 (1990).
10. B. Nandi, N. R. Das and S. N. Bhattacharyya, *Solvent Extr. Ion Exch.*, **1**, 141 (1983).
11. L. Delons, G. Picard and D. Tigreat, US Patent, 6,929,786 B2 (2005).
12. W. J. Kroll, A. W. Schleckten and L. A. Yerkes, *Trans. Electrochem. Soc.*, **89**, 263 (1946).
13. N. D. Denisova, E. K. Safronov, A. I. Pustil'nik and O. N. Bystrova, *Russ. J. Phys. Chem.*, **41**, 30 (1967).
14. M. L. Bromberg, US Patent, 2,852,446 (1958).
15. H. Ishikuza, Eur. Patent, 45270 (1982).
16. A. R. Cruz Duarte, M. M. Mooijer-van den Heuvel, C. M. M. Duarte and C. J. Peters, *Fluid Phase Equilib.*, **214**, 121 (2003).
17. R. P. Tangri, D. K. Bose and C. K. Gupta, *J. Chem. Eng. Data*, **40**, 823 (1995).
18. A. A. Palko, A. D. Ryan and D. W. Kuhn, *J. Phys. Chem.*, **62**, 319 (1958).
19. J. D. Kim and D. R. Spink, *J. Chem. Eng. Data*, **19**, 36 (1974).
20. H. Li, H. H. Nersisyan, K. T. Park, S. B. Park, J. G. Kim, J. M. Lee and J. H. Lee, *J. Nucl. Mater.*, **413**, 107 (2011).
21. C. C. Chen and P. M. Mathias, *AIChE J.*, **48**, 194 (2002).
22. J. R. Elliot and C. T. Lira, *Introductory chemical engineering thermodynamics*, Prentice-Hall Inc., NJ (1999).
23. J. K. Kim and M. S. Kim, *Fluid Phase Equilib.*, **238**, 13 (2005).
24. J. M. Lee, B. C. Lee and C. H. Cho, *Korean J. Chem. Eng.*, **17**, 510 (2000).
25. S. Yunhai, L. Honglai, W. Kun, X. Wende and H. Ying, *Fluid Phase Equilib.*, **234**, 1 (2005).
26. D. Y. Peng and D. B. Robinson, *Ind. Eng. Chem. Fundam.*, **15**, 59 (1976).
27. O. Annakou and P. Mitzey, *Heat Recov. Sys. CHP*, **15**, 241 (1995).
28. A. K. Jana, *Appl. Energy*, **87**, 1477 (2010).
29. J. M. Chew, C. C. S. Reddy and G. P. Rangaiah, *Chem. Eng. Process.*, **76**, 45 (2014).
30. N. V. D. Long and M. Y. Lee, *Energy*, **57**, 663 (2013).
31. A. A. Kiss, S. J. L. Landaeta and C. A. I. Ferreira, *Energy*, **47**, 531 (2012).